European Journal of Radiology 110 (2019) 233–241

Contents lists available at ScienceDirect

European Journal of Radiology

journal homepage: www.elsevier.com/locate/ejrad

Research article

Reorganization of brain networks following carotid endarterectomy: an exploratory study using resting state functional connectivity with a focus on the changes in Default Mode Network connectivity

Michele Porcu[a,*,1], Davide Craboledda[b,1], Paolo Garofalo[a], Luigi Barberini[c], Roberto Sanfilippo[b], Fulvio Zaccagna[d], Max Wintermark[e], Roberto Montisci[b], Luca Saba[a]

[a] Department of Radiology, University Hospital of Cagliari, Italy
[b] Department of Vascular Surgery, University Hospital of Cagliari, Italy
[c] Department of Medical Sciences and Public Health, University of Cagliari, Italy
[d] Department of Radiology, University of Cambridge School of Clinical Medicine, Cambridge, CB2 0QQ, UK
[e] Department of Radiology, Neuroradiology Division, Stanford University, Stanford, CA, USA

ARTICLE INFO

Keywords:
Resting-state functional connectivity MR
Carotid endarterectomy
Default mode network

ABSTRACT

Objectives: To assess whether there is mid-term reorganization in brain networks connectivity after Carotid Endarterectomy (CEA) using resting state functional connectivity Magnetic Resonance (fc-rsMR), with a special focus on the Default Mode Network (DMN).

Materials and methods: In this prospective exploratory study, 14 asymptomatic consecutive patients (10 males and 4 females, mean age 73.5) with unilateral, significant ICA stenosis eligible for CEA according to European Society for Vascular Surgery guidelines were prospectively recruited. The week before CEA procedure, each patient underwent both neurocognitive and rs-fcMR evaluations on the same day; the neurocognitive test consisted on a Mini Mental State Examination (MMSE). The same neurocognitive test and rs-fcMR examination were repeated on follow-up between 3–6 months after CEA. MMSE scores were compared using paired T-Student Test. Rs-fcMR Region Of Interest (ROI-to-ROI) and Seed-to-voxel group analysis were conducted using the CONN toolbox v18 and the SPM 12 software.

Results: Patients showed improvements in MMSE scores from before to after CEA (p-value = 0.0001). ROI-to-ROI analysis revealed several statistically significant connectivity changes following CEA, both in terms of positive and negative correlations; Seed-to-Voxel focusing on DMN revealed increased connectivity between medial prefrontal cortex (mPFC) and three different clusters of voxels.

Conclusions: CEA procedure is associated with an improvement in neurocognitive performance (according to MMSE testing) and reorganization of functional connectivity, including the DMN. These results represent a starting point in order to design further studies for a better understanding of the reorganization of brain networks following CEA, and to investigate the potential role of CEA as a therapeutic procedure for cognitive impairments in selected patients with critical ICA stenosis.

1. Introduction

Stroke is one of the leading causes of morbidity and mortality worldwide. In the first years of the 21st century, the age-standardized incidence of stroke in Europe was between 95–290 cases / 100,000 people per year, and it is estimated that by 2025 approximately 1.5 million people will suffer of stroke every year [1]. Large vessel atherosclerosis is an important risk factor for stroke and Transient Ischaemic Attack (TIA), in particular extracranial internal carotid artery atherosclerosis [2]. The recent European Society of Cardiology (ESC) guidelines on peripheral artery disease [3] report that 10–15% of all strokes are caused by thromboembolism from 50 to 99% stenosis of internal carotid arteries (ICA). According to these guidelines, ICA stenosis treatment is required to reduce risk of stroke/TIA, and the treatments of choice are Carotid Endarterectomy (CEA) and Carotid Artery Stenting (CAS), which should be considered for asymptomatic patients with

* Corresponding author at: Department of Medical Sciences and Public Health, University of Cagliari, S.S: 554, km 4,500 – CAP: 09042, Monserrato, Cagliari, Italy.
E-mail address: m.porcu@aoucagliari.it (M. Porcu).
[1] Contributed equally.

https://doi.org/10.1016/j.ejrad.2018.12.007
Received 16 July 2018; Received in revised form 22 October 2018; Accepted 6 December 2018
0720-048X/

60–99% stenosis and symptomatic patients with 50–99% stenosis. Plaque composition must be taken in count, even if its role still not standardized [4].

CEA is an open surgery technique, CAS is an endovascular technique, and both of them have their own advantages and disadvantages [3]. A recent meta-analysis by *Sardar P et al.* [5] showed that CEA and CAS showed similar rates of periprocedural death, stroke, myocardial infarction and non-periprocedural ipsilateral stroke, but the risk of long-term of overall stroke was lower in patients who underwent on CEA as compared to those who underwent CAS, even if CEA was associated with higher risk of facial nerve palsy and periprocedural myocardial infarction when compared to CAS.

It is also known that both asymptomatic and symptomatic carotid stenosis are associated with cognitive impairment, with chronic cerebral hypoperfusion and silent infarctions being the main responsible factors [6]. Different studies using various neurocognitive tests investigated the effects of CEA and/or CAS [7–12] and suggest that these procedures are associated with an improvement in cognitive performance in the short- and long-term (between 3 months and 3 years depending on the study).

Resting-state functional connectivity Magnetic Resonance (rs-fcMR) is an MR technique used to study the brain function in humans. It relies on blood-oxygen level-dependent (BOLD) signal differences generated by spontaneous neuronal activity during resting state [13]. Some researchers already applied this technique to study functional connectivity in patients with asymptomatic ICA stenosis [14–17], and to assess the effects of CAS and aggressive medical therapy [18,19]. In particular, *Lin C-J et al.* [14] demonstrated that patients with asymptomatic unilateral ICA stenosis (≥ 70%) showed reduced connectivity in different brain networks including the Default Mode Network (DMN), a well-known and defined brain network activated in the resting state, when a person is not focusing on the outside world but just resting [20,21]). Another study showed that DMN showed increased connectivity following CAS [18].

In this exploratory study, we investigated the mid-term effects of CEA both on cognitive function using a neuropsychological test and resting state functional connectivity changes, focusing in particular on the connectivity of DMN.

2. Materials and methods

The study was designed as a prospective pilot study; according to its exploratory intent, its intent was to recruit at least 12 consecutive patients, according to *Joulious SA* [22]. The ethical committee approved the study. All the patients gave their written informed consent before enrollment. Fourteen consecutive asymptomatic patients, 10 males and 4 females (age between 65 and 82 years; mean age: 73.5 years; mean age for male group: 74.4 years; mean age for female group: 71.25 years) were recruited between January 2017 and December 2017 at the University Hospital of Cagliari (Italy) (Table 1). All the patients had a unilateral ICA stenosis with surgical indication for CEA according to the guidelines of the European Society for Vascular Surgery [23]. Exclusion criteria were as follows: a) patients who were not right-hand dominant; b) severe systemic inherited or acquired diseases in medical history (in particular history of severe psychiatric/neurological conditions and/or major stroke), except cognitive dysfunction; c) contraindications to MR examinations; d) presence of functional disability (values ≥2 according to modified Rankin scale [24]); e) patients with significant pathology revealed during MR examination.

All the patients undeerwent the Italian version of Mini Mental State Examination (MMSE) corrected according to age and schooling [25,26] in the week prior to the CEA. On the same day, a non-contrast rs-fcMR scan was performed using a 1.5 T (peak amplitude 33 m T/m, slew rate 160 m T/m/ms) Philips "Achieva dStream" scanner (Philips, Best, Netherland), with a 32 channels head coil.

The dedicated MR scan protocol included three sequences: a) a 3D Fluid Attenuated Inversion Recovery (FLAIR), TE = 292.283 ms, TR = 4800 ms, Inversion Time = 1660 ms, flip angle 90°, slice thickness = 1 mm); b) a structural 3D T1-weighted Turbo Field Echo (TFE) (TE = 3.43 ms, TR = 7.5 ms, flip angle = 8°, slice thickness = 1 mm, spacing between slices = 1 mm); c) a resting state functional T2 weighted Echo-Planar Imaging (EPI) sequence (TE = 50 ms; TR = 3000 ms; flip angle = 90°; slice thickness = 5 mm; matrix: 80 × 80; volumes acquired: 326). Patients were accurately instructed by a radiologist to follow technologist's instructions during MR examination, and the recommendation of not thinking neither sleeping was given to them by the radiologist before the beginning of the resting state EPI sequence.

Table 1
Demographic data of the study population.

Patients	Age at the moment of recruitment	Sex	Side treated	MMSE* score before CEA	MMSE* score after CEA
Patient 1	72	Male	Left	27.7	27.7
Patient 2	65	Male	Right	18.9	22.9
Patient 3	76	Female	Left	24.3	25
Patient 4	76	Female	Right	26	26
Patient 5	75	Male	Left	22	28
Patient 6	72	Female	Left	12.7	23.7
Patient 7	77	Male	Right	24	26
Patient 8	80	Male	Right	22.4	28.4
Patient 9	81	Male	Right	18.4	27.4
Patient 10	70	Male	Left	20.4	23.4
Patient 11	82	Male	Left	14.4	20.4
Patient 12	76	Male	Right	22.3	24.7
Patient 13	61	Female	Right	20	23.7
Patient 14	66	Male	Left	16	20.4

The presence of significant pathology such as acute lacunar and/or territorial infarction, chronic territorial infarction or other incidental findings like intra- or extra-axial neoplastic lesions, inflammatory or infective diseases, was ruled out in all patients. On the contrary, the presence of hyperintense lesions on FLAIR sequences suggestive for leukoaraiosis and/or chronic lacunar infarctions was not considered an exclusion criterion because they are common findings in patients with significant ICA stenosis and they are often clinically asymptomatic [27]. All the scans were interpreted negative for the presence of significant pathology, and no subjects were excluded from the analysis.

None of the patients suffered any procedural or peri-procedural complications after CEA, and the clinical course was uneventful. A follow-up MMSE and MR scan using the same protocol were performed on the same day between 3 and 6 months after surgical procedure (mean follow-up time: 4.2 months); the MRI examinations did not reveal any morphological change of brain structures (for example ischemic infarction) when compared to the baseline MRI. Both the baseline and follow-up MR examinations were analyzed by two neuroradiologists (MP and PG, 5 and 4 years of radiological experience, respectively).

2.1. MMSE scores analysis

The normal distribution of the Pre-CEA and Post-CEA MMSE scores was tested using the Kolmogorov-Smirnov Z test, with the statistically significance threshold set at a p-value < 0.2. The Pre-CEA and Post-CEA MMSE scores were then compared using paired samples *t*-tests, and a p-value threshold < 0.05 was considered for statistically significance. All p-values were calculated using a two-tailed significance level. Both the Kolmogorov-Smirnov Z tests and the paired samples *t*-test were performed with the SPSS 24 statistical package (SPSS Inc, Chicago, IL).

2.2. Rs-fcMR analysis

The connectivity analysis was performed with the CONN-fMRI fc

toolbox v18a [28] in conjunction with SPM 12 (Wellcome Department of Imaging Neuroscience, London, UK; http://www.fil.ion.ucl.ac.uk/spm/). The CONN toolbox is able to perform seed-based correlation analysis according to the low-frequency, temporal fluctuations of BOLD signals. All the structural and functional sequences (14 pre-CEA and 14 post-CEA) were preprocessed using the CONN's default pipeline for volume-based analysis following these steps:

1 Functional realignment and unwarping (subject motion estimation and correction);
2 Functional center to (0,0,0) coordinates (translation);
3 Functional slice-timing correction ;
4 Functional outlier detection using intermediate settings, i.e. 97th percentile in normative sample in functional outlier detection system with Global-signal z-value threshold = 5 and Subject-motion mm threshold = 0.9
5 Functional direct segmentation (simultaneous grey matter / white matter / cerebrospinal fluid) and normalization to Montreal Neurological Institute (MNI) adopting default Tissue Probability Maps with target resolution = 2 mm;
6 Structural center to (0,0,0) coordinates (translation);
7 Structural segmentation (simultaneous grey matter / white matter / cerebrospinal fluid) and normalization to MNI space adopting default Tissue Probability Maps with target resolution = 2 mm;
8 Functional smoothing (8 mm full width half maximum Gaussian kernel filter).

Similarly to Rongfeng et al. [29], the first 10 volumes of functional sequences were excluded from analysis so that magnetization could reach steady state and patients could adapt to the MR scanner noise. Further, similarly to Fallon et al. [30] a motion artefact threshold (translation > 3 mm, rotation > 1°) was applied as exclusion criteria to motion parameters derived from realignment, but no patients displayed gross movements and therefore no patients were excluded from the analysis. BOLD signals from ventricular system and cerebral white matter were removed exploiting the principal component analysis of multivariate BOLD signal within each of these masks [28].

Subsequently, BOLD data underwent a denoising process applying a band-pass filter (0.008 to 0.09 Hz) in order to reduce both noise effects and low frequency drift.

Two different rs-fcMR analyses were then performed: a) Regions of Interest to Region of Interest (ROI-to-ROI) and b) Seed-to-Voxel analysis. For both the Seed-to-Voxel and ROI-to-ROI analyses, individual correlation maps throughout the whole brain were generated extracting the mean resting-state BOLD time course from each single seed (in terms of ROI) and calculating the correlation coefficients with the BOLD time-course of each voxel (Seed-to-Voxel) or other seeds (ROI-to-ROI). These correlations were obtained by applying the General Linear Model (GLM) and bivariate correlation analysis weighted for Haemodynamic Response Function (HRF): higher Z-scores indicate positive correlations between ROIs, (i.e. increased functional connectivity reflected by increased BOLD signal time series synchronization), whereas lower Z-scores indicate negative correlations (i.e. decreased connectivity and decreased synchronicity between or between different ROIs or ROIs and voxels). Fisher's transformation was then applied to all Z-scores derived from bivariate correlations, and correlation coefficients were converted into standard scores. These maps were obtained in the first-level analysis of the CONN's pipeline adopting CONN's default atlas for the definition of ROIs: cortical and subcortical ROIs referred to the Harvard-Oxford atlas [31–34]; cerebellar ROIs according to the Automated Anatomical Labeling (AAL) atlas [35]; DMN seed ROIs consisted of 10 mm diameter spheres and were defined similarly to *Fallon N et al.* [30] according to a meta-analysis of DMN functional MR studies by Laird et al. [36]: precuneus (pC), posterior cingulate cortex (PCC), ventral anterior cingulate cortex (vACC), medial prefrontal cortex (mPFC), left middle frontal gyrus (L.MFG), bilateral inferior parietal lobule (R/L.IPL) and bilateral middle temporal gyrus (R/L.MTG) (Table 2).

Table 2
MNI (x,y,z) co-ordinates of seed ROIs for DMN [30].

Regions of DMN	MNI coordinates (mm)		
	x	y	z
Precuneus (pC)	−4	−58	44
Posterior cingulate cortex (PCC)	−4	−52	22
Ventral anterior cingulate cortex (vACC)	2	32	−8
Medial prefrontal cortex (mPFC)	−2	50	18
Left middle frontal gyrus (L.MFG)	−26	16	44
Right middle temporal gyrus (R.MTG)	46	−66	16
Left middle temporal gyrus (L.MTG)	−42	−66	18
Right inferior parietal lobule (R.IPL)	52	−28	24
Left inferior parietal lobule (L.IPL)	−56	−36	28

In the second level analysis of the Conn's pipeline (group analysis), the differences of connectivity between pre-CEA and post-CEA group connectivity were measured applying paired T-tests. For the ROI-to-ROI analysis, p-FDR was set < 0.05 to determine significant correlations between the components of the DMN and the rest of the brain. Similarly to previous studies [30,37–39], for the Seed-to-Voxel analysis, voxel-wise statistics throughout the entire brain was performed for every seed ROI of the DMN choosing p-uncorrected value < 0.001 before applying a False Discovery Rate correction to p-value (p-FDR < 0.05).

3. Results

3.1. MMSE scores analysis

The Kolmogorov-Smirnov Z tests confirmed the normal distribution of both the Pre-CEA and Post-CEA MMSE scores (Pre-CEA MMSE scores' p-value = 0.120, Post-CEA MMSE scores' p-value = 0.124) (Table 3 and Fig. 1a and b). The comparison of the pre- and post-CEA MMSE scores showed a statistically significant improvement of the cognitive performance after CEA (p = 0.001) (Table 4 and Fig. 1c).

3.2. Rs-fcMR analysis

In ROI-to-ROI analysis, when all the cortical, subcortical and cerebellar ROIs of the default CONN's atlas (but not those of DMN's components) were considered together, 29 statistical significant connectivity changes throughout the brain were found (27 positive and 2 negative correlations) (Table 5 and Fig. 2). When DMN's ROI's were inserted in the analysis, mPFC showed statistically significant increased synchronicity after CEA in the right Cerebellum Crus 1 and in both the right and left Cerebellum Crus 2 (Table 6 and Fig. 3); no other DMN seeds showed statistically significant connectivity changes.

The Seed-to-Voxel analysis revealed that patients after CEA showed different significant connectivity changes between DMN seed mPFC, with three different clusters of cortical regions, named A, B and C (Table 7 and Fig. 4). In cluster A (size of contiguous voxels = 192; p-FDR = 0.0006876), mPFC showed increased connectivity with the

Table 3
Kolmogorov-Smirnov tests confirmed the normal distribution of both Pre-CEA and Post-CEA MMSE scores (df = degree of freedom).

Test of Normality - Kolmogorov-Smirnov[a]			
	Statistic	df	P-value
Pre-CEA MMSE scores	0.120	14	0.200
Post-CEA MMSE scores	0.124	14	0.200

*This is a lower bound of the true significance.
[a] Lilliefors Significance Correction.

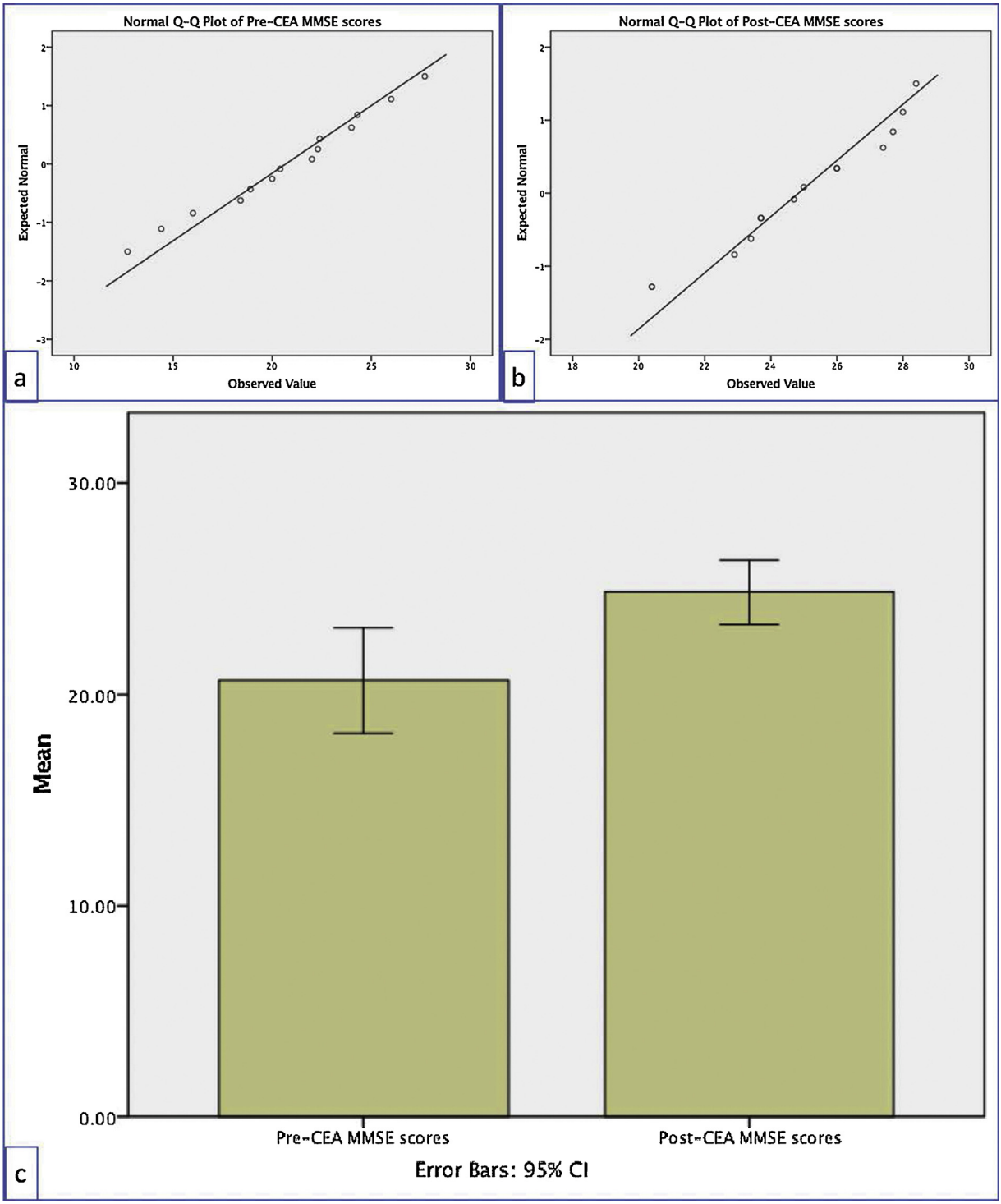

Fig. 1. Kolmogorov-Smirnov and Student T-tests for the evaluation of paired MMSE scores. a) Normal Q-Q plot of Pre-CEA MMSE scores; b) Normal Q-Q plot of Post-CEA MMSE scores; c) results of Student T-tests for paired values.

Precuneus (cortical region derived from the Harvard-Oxford atlas [31–34], but not with the DMN seeds [30,36]); in cluster B (size of contiguous voxels = 112; p-FDR = 0.048661), mPFC showed increased connectivity with the with the right Cerebellum Crus 1, with both the right and left Cerebellum Crus 2, and with the Vermis 7, similarly to what observed in ROI-to-ROI analysis; in cluster C (size of contiguous voxels = 104; p-FDR = 0.048661) mPFC showed increased connectivity with the right middle and superior frontal gyri. Also in this case, no other DMN seeds showed statistically significant connectivity changes.

4. Discussion

In our study, we found that patients who underwent CEA showed improvements in MMSE scores and rreorganization of their cerebral circuits as defined by rs-fcMR. Improvements in MMSE scores are in agreement with a trend well demonstrated in the literature [7–12]. The concept underlying this study is that intracerebral blood flow dynamic changes following CEA result in changes in resting state functional connectivity that may lead to improvement in the neurocognitive performance.

Table 4
Student T-tests for paired values showing improvement of MMSE scores after CEA (p-value = 0.0001), with a Pre-CEA mean average score of 20.67 and Post-CEA mean average score of 24.83 (N = number of samples; Std deviation = Standard deviation; Std Error mean = Standard error of the mean; t = t-value; df = degree of freedom).

Paired Samples Statistics			
	Mean	N	Std deviation	Std Error mean
Post-CEA MMSE	20.67	14	4.32	1.15
Post-CEA MMSE scores	24.83	14	2.60	0.69

Paired Samples Correlations			
	N	Correlation	P-value
Post-CEA MMSE and Post-CEA MMSE scores	14	0.665	0.09

Paired Samples Test Pre-CEA and Post-CEA MMSE scores								
	Mean	Std. deviation	Std. Error mean	95% Confidence Interval of the Difference		t	df	p-value (2-tailed)
				Lower	Upper			
Post-CEA MMSE and Post-CEA MMSE scores	−4.15	3.23	0.86	−6.02	−2.28	−4.80	13	0.0001

Table 5
Positive and negative correlations derived from ROI-to-ROI analysis (aPaHC = anterior division of parahippocampal cortex; aSMG = anterior division of supramarginal gyrus; CO = central opercular cortex; PreCG = precentral Gyrus; PP = planum polare; PO = parietal operculum cortex; FP = Frontal pole; Ver = vermis; AC = anterior division of cingulate gyrus; PC = posterior division of cingulate gyrus; IC = insular cortex; TP = temporal pole; PaCiG = paracingulate gyrus; MidFG = middle frontal gyrus; pPaHC = posterior division of parahippocampal gyrus; pMTG = posterior division of middle temporal gyrus; sLOC = superior division of lateral occipital cortex; HG = Heschl's gyrus; Caudate = Caudate; Putamen = Putamen; Amygdala = Amygdala; r = right; l = left).

Positive correlations			
Analysis Unit	Statistic	p-unc	p-FDR
aPaHC r -aSMG r	T(13) = 5.59	0.0001	0.0066
aPaHC r -CO r	T(13) = 5.50	0.0001	0.0066
PreCG l -PP l	T(13) = 5.71	0.0001	0.0094
PP l -PreCG l	T(13) = 5.71	0.0001	0.0094
aSMG r -aPaHC r	T(13) = 5.59	0.0001	0.0115
aPaHC r -PO r	T(13) = 4.94	0.0003	0.0118
CO r -aPaHC r	T(13) = 5.50	0.0001	0.0133
FP l -Ver6	T(13) = 5.32	0.0001	0.0183
Ver6 -FP l	T(13) = 5.32	0.0001	0.0183
PC -AC	T(13) = 5.28	0.0001	0.0194
AC -PC	T(13) = 5.28	0.0001	0.0194
Putamen l-IC r	T(13) = 5.24	0.0002	0.0210
IC r -Putamen l	T(13) = 5.24	0.0002	0.0210
TP r -Ver8	T(13) = 5.08	0.0002	0.0275
Ver8 -TP r	T(13) = 5.08	0.0002	0.0275
PC -PaCiG r	T(13) = 4.53	0.0006	0.0293
PC -FP r	T(13) = 4.44	0.0007	0.0293
PO r -aPaHC r	T(13) = 4.94	0.0003	0.0341
PO r -aPaHC l	T(13) = 4.37	0.0008	0.0341
PO r -TP r	T(13) = 4.35	0.0008	0.0341
PaCiG r -PC	T(13) = 4.53	0.0006	0.0372
PaCiG r - MidFG r	T(13) = 4.53	0.0006	0.0372
pPaHC r -pMTG r	T(13) = 4.91	0.0003	0.0374
pMTG r -pPaHC r	T(13) = 4.91	0.0003	0.0374
Amygdala r-Caudate r	T(13) = -4.91	0.0003	0.0375
aPaHC r -sLOC r	T(13) = 4.08	0.0013	0.0420
aPaHC r -PO l	T(13) = 3.97	0.0016	0.0420

Negative correlations			
Analysis Unit	Statistic	p-unc	p-FDR
Caudate r - Amygdala r	T(13) = -4.91	0.0003	0.0375
Caudate r - HG r	T(13) = -4.50	0.0006	0.0391

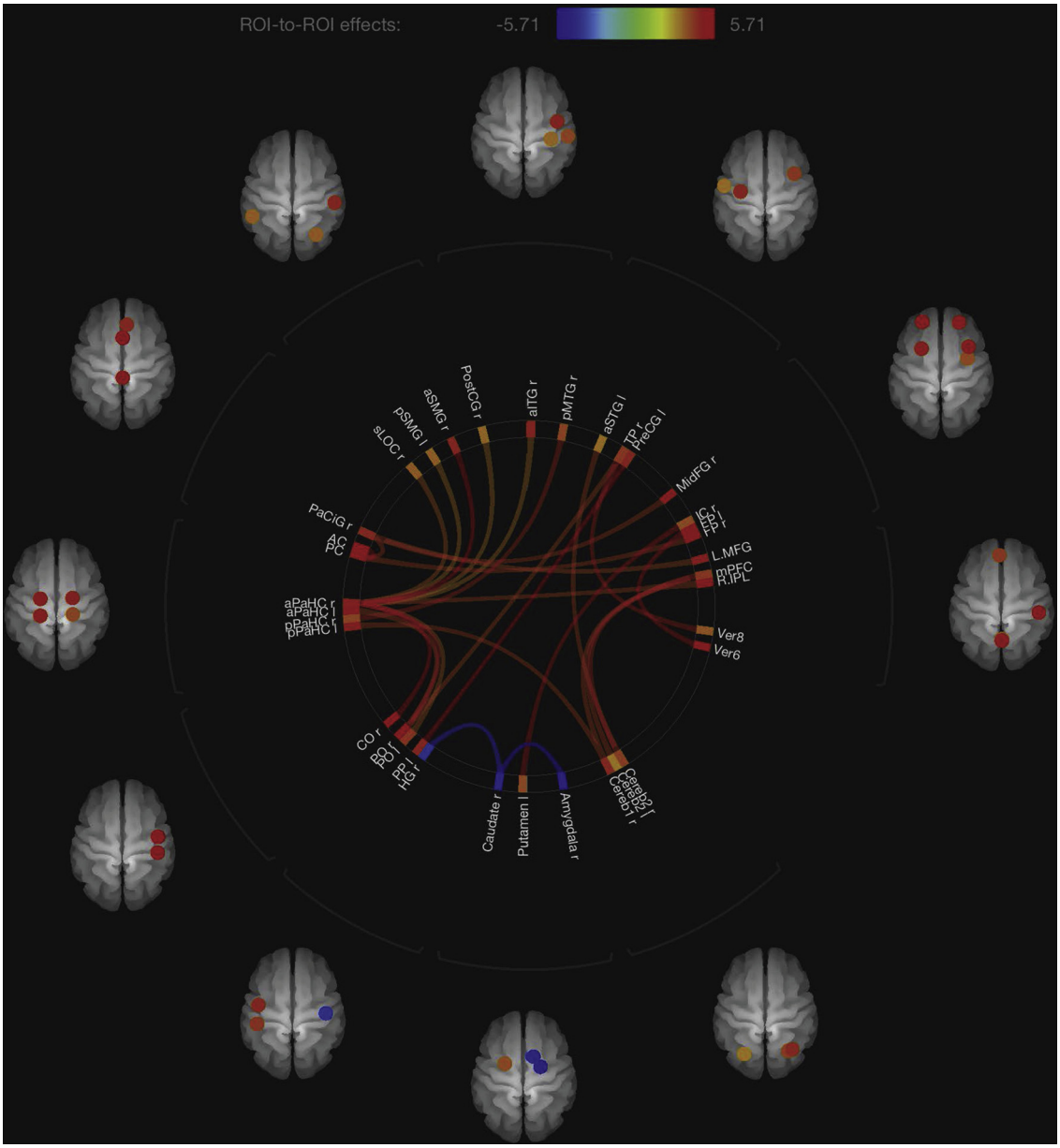

Fig. 2. CEA procedure is associated with a reorganization of brain networks in terms of both multiple positive and negative correlations, as evidenced in this "connectome ring".

In 2010, Schaaf et al. [37] studied the effects of CEA on functional MR, demonstrating that BOLD signal changes immediately after CEA reflect ameliorated cerebrovascular reactivity, but they did not focus on brain network changes on rs-fcMR. To our knowledge, this is the first rs-fcMR study performed in patients who underwent CEA procedure: differences in resting state functional connectivity were found after CEA, similarly to the differences observed in a different study after CAS [19]. The ROI-to-ROI analysis revealed statistically significant changes

Table 6
mPFC positive correlations as revealed in ROI-to-ROI analysis (p-unc = uncorrected p-value; p-FDR = False Discovery Rate corrected p-value).

Seed	Statistic	p-unc	p-FDR
Seed mPFC	F(3) (11) = 11.68 Intensity = 13.88 Size = 3	0.0010	0.0010

Connections	Statistic	p-unc	p-FDR
mPFC-Cereb2 r	T(13) = 4.91	0.0003	0.0300
mPFC-Cereb2 l	T(13) = 4.51	0.0003	0.0300
mPFC-Cereb1 r	T(13) = 4.46	0.0006	0.0300

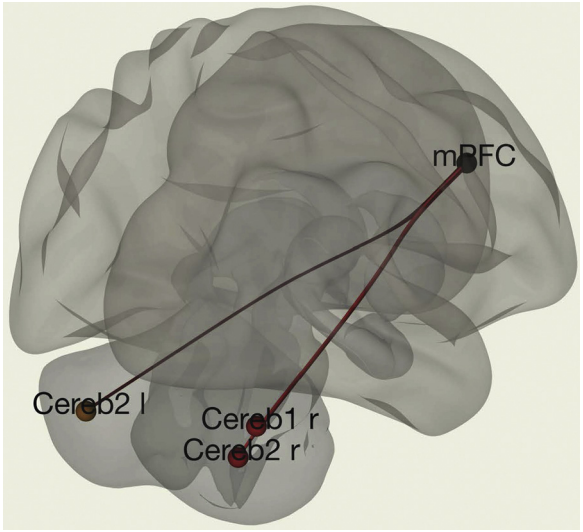

Fig. 3. ROI-to-ROI image showing positive correlations between medial prefrontal cortex (mPFC) and right cerebellar crus I (Cereb 1 r) and right (Cereb 2 r) and left (Cereb 2 l) cerebellar crus 2.

in brain connectivity changes following CEA, and It is reasonable to envision that the increase in cerebral blood flow following CEA can lead to a reorganization of the cerebral circuits in the mid-term. In addition, based on the results of MMSE test, this reorganization may be related to the observed cognitive improvement.

DMN is one of the most studied cerebral network, and recent researches demonstrate it being involved in cognition [20,21], in particular self-generated thoughts [38]. For example, a study by Konishi et al. [39] suggests that DMN could be implied in higher order thoughts (such as imagining the future or considering the perspective of another person) because it allows cognition to be shaped by information from stored representations. Another study by *Smith V et al.* [40] suggested that the DMN could encode a scene, episode or context by integrating spatial, self-referential, and temporal information. According also to the findings of Lin et al. [14,18], we hypothesized that DMN could be involved in the reorganization of brain networks following CEA, partly explaining the cognitive improvements observed in these patients. Seed-to-Voxel analysis focused on DMN seeds evidenced a greater connectivity of mPFC with other cerebral and cerebellar regions: in particular three clusters (named A, B and C) showed increased connectivity with mPFC.

Cluster A, the biggest one, consists mainly of voxels from the precuneus, another DMN network region. Looking carefully at our results, one could argue that mPFC showed increased connectivity with the precuneus ROI derived from the CONN's default Harvard-Oxford atlas [31–34] but not with that defined by Laird et al. [36]. This incongruence reflects an ongoing debate about the exact definition of theDMN network ROIs, and it is reasonable to think that there is a real incremented connectivity between those two areas of DMN despite this incongruence.

Cluster B consists mainly of voxel from the cerebellum, in particular Crus I and II, and these results were also confirmed in the ROI-to-ROI analysis. These results are aligned with the evidence that there is a cerebro-cerebellar connection between mPFC and cerebellar region Crus I and II [41].

Cluster C, the smallest one, consisted mainly of voxels within the right middle and superior frontal gyri. These areas are considered part of the mPFC, and one possible explanation could be that the same areas within the mPFC may become hyperconnected.

As mentioned in the introduction, previous studies showed that patients with asymptomatic ICA stenosis demonstrate reduced connectivity in different brain networks including the Default Mode

Table 7
Clusters of voxels showing increased connectivity with mPFC in Seed-to-Voxel analysis (p-FWE = Family Wise Error corrected p-value; p-unc = uncorrected p-value; p-FDR = False Discovery Rate corrected p-value).

Cluster name	Clusters according to MNI space (x, y, z)	size	Coverage	Size p-FWE	Size p-FDR	Size p-unc	Peak p-FWE	Peak p-unc
A	−08 −58 + 62	192	● 180 voxels covering 3% of atlas.Precuneous (Precuneous Cortex) ● 3 voxels covering 0% of atlas.sLOC l (Lateral Occipital Cortex, superior division Left) ● 2 voxels covering 0% of atlas.SPL l (Superior Parietal Lobule Left) ● 1 voxels covering 0% of atlas.sLOC r (Lateral Occipital Cortex, superior division Right) ● 6 voxels covering 0% of atlas.not-labeled	0.003143	0.006876	0.000111	0.847543	0.000018
B	+08 −80 −30	112	● 66 voxels covering 3% of atlas.Cereb2 r (Cerebellum Crus2 Right) ● 24 voxels covering 1% of atlas.Cereb1 r (Cerebellum Crus1 Right) ● 18 voxels covering 1% of atlas.Cereb2 l (Cerebellum Crus2 Left) ● 4 voxels covering 2% of atlas.Ver7 (Vermis 7)	0.047998	0.048661	0.001733	0.898679	0.000024
C	+32 + 14 + 42	104	● 42 voxels covering 2% of atlas.MidFG r (Middle Frontal Gyrus Right) ● 25 voxels covering 1% of atlas.SFG r (Superior Frontal Gyrus Right) ● 37 voxels covering 0% of atlas.not-labeled	0.064644	0.048661	0.002355	0.975835	0.000049

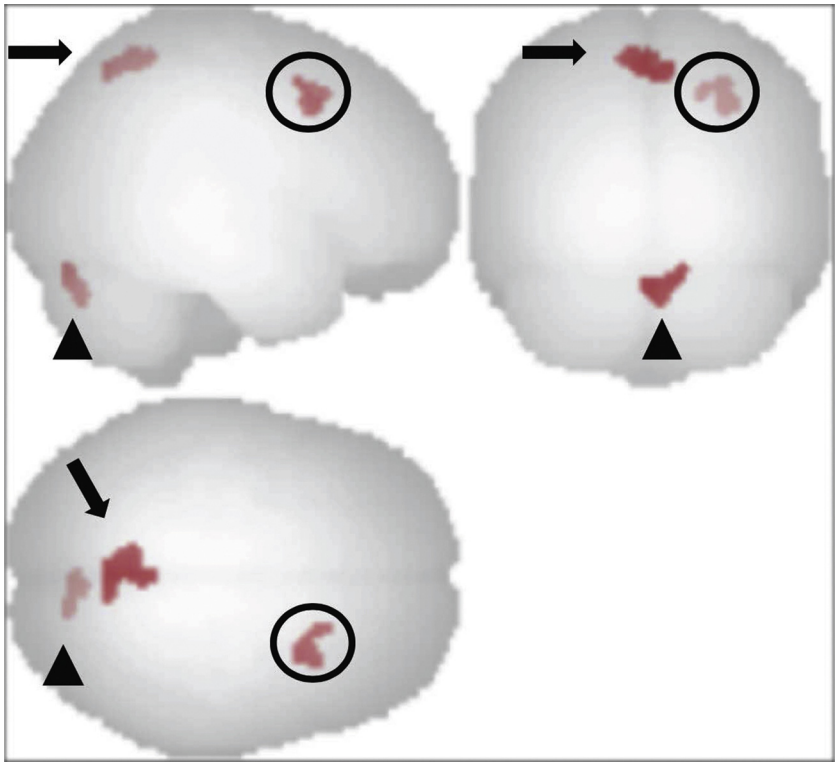

Fig. 4. Seed-to-voxel analysis demonstrating increased connectivity of mPFC with cluster A (arrow), cluster B (arrowheads) and cluster C (circle) after CEA.

Network (DMN) [14,17]. To the best of our knowledge, no study investigated the effects of CEA on brain networks using rs-fcMR, and our results can be only compared to those obtained in patients who underwent CAS. It is interesting to observe that a previous study by Lin et al. [18] revealed that mPFC showed increased connectivity with posterior prefrontal cortex following CAS combined with aggressive medical therapy. Even if the design of these studies differ from one another, it is reasonable to hypothesize a pivotal role for the DMN, and in particular the mPFC, in the reorganization of the cerebral circuits after ICA revascularization, independently from the technique adopted (CEA or CAS). The mPFC is involved in cognitive control [42], and increased connectivity of this region with other brain's areas could explain the improved MMSE scores observed in our study. According to the important number of brain connections identified in the ROI-to-ROI analysis, the reorganization may affect not only the cognitive sphere, but also other human brain functions such as memory, behaviour and motion.

We ackowledge three major limitations to our analysis. The first one is the small number of patients invluded in this study: the study was designed as exploratory, because of the lack of any previous longitudinal study investigating the effects of CEA on rs-fcMR. The first goal was to assess whether there was any brain connectivity changes after CEA. The second limitation is the absence of comparison with healthy controls, but previous studies [14–17] already demonstrated different connectivity patterns between patients with severe asymptomatic carotid stenosis and healthy controls on rs-fcMR. The third limitation relates to the lack of an integrated and more specific neuropsychological analysis: we justify this choice on the basis that previous studies already demonstrated improvements in neurocognitive performances following CEA [7–12], and since the research was designed as exploratory, we used MMSE as a surrogate test for the evaluation of neurocognitive performance.

5. Conclusions

Our exploratory study showed the presence of the mid-term reorganization of several functional connectivity networks following CEA, some of them involving DMN (in particular mPFC), and this reoagnization may explain the neurocognitive improvements seen after the surgical intervention. Our pilot study should be considered a starting point for further studies using wider populations and different neurocognitive and psychological tests in order to better understand the correlation between brain network changes and neurocognitive effects following CEA. It could represent a starting point to redefine the role of CEA not only as a procedure for the prevention of stroke, but also for the therapy for neurocognitive impairment in patients with critical ICA stenosis.

Conflict of interest

The authors declare that they have no conflict of interest.

Ethical approval

All procedures performed in the studies involving human participants were in accordance with the ethical standards of the institutional and/or national research committee and with the 1964 Helsinki Declaration and its later amendments or comparable ethical standards.

Funding

No funding was received for this study.

References

[1] Y. Béjot, H. Bailly, J. Durier, M. Giroud, Epidemiology of stroke in Europe and trends for the 21st century, Presse Med. 45 (December (12 Pt 2)) (2016) e391–e398, https://doi.org/10.1016/j.lpm.2016.10.003 Epub 2016 Nov 2. PubMed PMID: 27816343.

[2] M.L. Flaherty, B. Kissela, J.C. Khoury, et al., Carotid artery stenosis as a cause of stroke, Neuroepidemiology. 40 (1) (2013) 36–41, https://doi.org/10.1159/000341410.

[3] V. Aboyans, J.B. Ricco, M.E.L. Bartelink, M. Björck, M. Brodmann, T. Cohnert, J.P. Collet, M. Czerny, M. De Carlo, S. Debus, C. Espinola-Klein, T. Kahan,

S. Kownator, L. Mazzolai, A.R. Naylor, M. Roffi, J. Röther, M. Sprynger, M. Tendera, G. Tepe, M. Venermo, C. Vlachopoulos, I. Desormais, ESC Scientific Document Group, ESC Guidelines on the Diagnosis and Treatment of Peripheral Arterial Diseases, in collaboration with the European Society for Vascular Surgery (ESVS): document covering atherosclerotic disease of extracranial carotid and vertebral, mesenteric, renal, upper and lower extremity arteries endorsed by: the European Stroke Organization (ESO) the Task Force for the Diagnosis and Treatment of Peripheral Arterial Diseases of the European Society of Cardiology (ESC) and of the European Society for Vascular Surgery (ESVS), Eur. Heart J. 2017 (August) (2017), https://doi.org/10.1093/eurheartj/ehx095 [Epub ahead of print] PubMed PMID: 28886620.

[4] L. Saba, C. Yuan, T.S. Hatsukami, N. Balu, Y. Qiao, J.K. DeMarco, T. Saam, A.R. Moody, D. Li, C.C. Matouk, M.H. Johnson, H.R. Jäger, M. Mossa-Basha, M.E. Kooi, Z. Fan, D. Saloner, M. Wintermark, D.J. Mikulis, B.A. Wasserman, Vessel wall imaging study group of the american society of neuroradiology. carotid artery wall imaging: perspective and guidelines from the asnr vessel wall imaging study group and expert consensus recommendations of the american society of neuroradiology, AJNR Am. J. Neuroradiol. 39 (February (2)) (2018) E9–E31, https://doi.org/10.3174/ajnr.A5488 Epub 2018 Jan 11. PubMed PMID: 29326139.

[5] P. Sardar, S. Chatterjee, H.D. Aronow, A. Kundu, P. Ramchand, D. Mukherjee, R. Nairooz, W.A. Gray, C.J. White, M.R. Jaff, K. Rosenfield, J. Giri, Carotid artery stenting versus endarterectomy for stroke prevention: a meta-analysis of clinical trials, J. Am. Coll. Cardiol. 69 (May (18)) (2017) 2266–2275, https://doi.org/10.1016/j.jacc.2017.02.053 PubMed PMID: 28473130.

[6] T. Wang, B. Mei, J. Zhang, Atherosclerotic carotid stenosis and cognitive function, Clin. Neurol. Neurosurg. 146 (July) (2016) 64–70, https://doi.org/10.1016/j.clineuro.2016.03.027 Epub 2016 Apr 20. Review. PubMed PMID: 27152468.

[7] J. Watanabe, T. Ogata, T. Higashi, T. Inoue, Cognitive change 1 year after CEA or CAS compared with medication, J. Stroke Cerebrovasc. Dis. 26 (June (6)) (2017) 1297–1305, https://doi.org/10.1016/j.jstrokecerebrovasdis.2017.01.024 Epub 2017 Feb 22. PubMed PMID: 28236597.

[8] M.G. Carta, M.E. Lecca, L. Saba, R. Sanfilippo, E. Pintus, M. Cadoni, F. Sancassiani, M.F. Moro, D. Craboledda, C. Lo Giudice, G. Finco, M. Musu, R. Montisci, Patients with carotid atherosclerosis who underwent or did not undergo carotid endarterectomy: outcome on mood, cognition and quality of life, BMC Psychiatry 12 (November (15)) (2015) 277, https://doi.org/10.1186/s12888-015-0663-y PubMed PMID: 26563766; PubMed Central PMCID: PMC4642779.

[9] S. Lattanzi, L. Carbonari, G. Pagliariccio, M. Bartolini, C. Cagnetti, G. Viticchi, L. Buratti, L. Provinciali, M. Silvestrini, Neurocognitive functioning and cerebrovascular reactivity after carotid endarterectomy, Neurology 90 (January (4)) (2018) e307–e315, https://doi.org/10.1212/WNL.0000000000004862 Epub 2017 Dec 27. PubMed PMID: 29282326.

[10] G.M. Shi, T. Jiang, H. Zhang, M.H. Li, M. Wang, Y.K. Liu, H.C. Shi, F. Zhou, Q. Huang, L.Y. Zhang, J.S. Zhou, Y.D. Zhang, Carotid endarterectomy and carotid artery stenting lead to improved cognitive performance in patients with severe carotid artery stenosis, Curr. Neurovasc. Res. 13 (1) (2016) 45–49 PubMed PMID: 26666638.

[11] P. Kougias, R. Collins, N. Pastorek, S. Sharath, N.R. Barshes, K. McCulloch, G. Pisimisis, D.H. Berger, Comparison of domain-specific cognitive function after carotid endarterectomy and stenting, J. Vasc. Surg. 62 (August (2)) (2015) 355–361, https://doi.org/10.1016/j.jvs.2015.02.057 PubMed PMID: 26211378.

[12] L. Picchetto, G. Spalletta, B. Casolla, C. Cacciari, M. Cavallari, C. Fantozzi, A. Ciuffoli, M. Rasura, F. Imperiale, G. Sette, C. Caltagirone, M. Taurino, F. Orzi, Cognitive performance following carotid endarterectomy or stenting in asymptomatic patients with severe ICA stenosis, Cardiovasc. Psychiatry Neurol. 2013 (2013) 342571, https://doi.org/10.1155/2013/342571 Epub 2013 Dec 21. PubMed PMID: 24455200; PubMed Central PMCID: PMC3880731.

[13] B.R. Buchbinder, Functional magnetic resonance imaging, Handb. Clin. Neurol. 135 (2016) 61–92, https://doi.org/10.1016/B978-0-444-53485-9.00004-0 Review. PubMed PMID: 27432660.

[14] C.-J. Lin, P.-C. Tu, C.-M. Chern, et al., Connectivity features for identifying cognitive impairment in presymptomatic carotid stenosis. Yu C, ed, PLoS One 9 (1) (2014) e85441, , https://doi.org/10.1371/journal.pone.0085441.

[15] T.Y. Chang, K.L. Huang, M.Y. Ho, P.S. Ho, C.H. Chang, C.H. Liu, Y.J. Chang, H.F. Wong, I.C. Hsieh, T.H. Lee, H.L. Liu, Graph theoretical analysis of functional networks and its relationship to cognitive decline in patients with carotid stenosis, J. Cereb. Blood Flow Metab. 36 (April (4)) (2016) 808–818, https://doi.org/10.1177/0271678X15608390 Epub 2015 Oct 1. PubMed PMID: 26661184; PubMed Central PMCID: PMC4820004.

[16] H.L. Cheng, C.J. Lin, B.W. Soong, P.N. Wang, F.C. Chang, Y.T. Wu, K.H. Chou, C.P. Lin, P.C. Tu, I.H. Lee, Impairments in cognitive function and brain connectivity in severe asymptomatic carotid stenosis, Stroke. 43 (October (10)) (2012) 2567–2573 Epub 2012 Aug 30. PubMed PMID: 22935402.

[17] T. Wang, F. Xiao, G. Wu, J. Fang, Z. Sun, H. Feng, J. Zhang, H. Xu, Impairments in brain perfusion, metabolites, functional connectivity, and cognition in severe asymptomatic carotid stenosis patients: an integrated MRI study, Neural Plast. 2017 (2017) 8738714, , https://doi.org/10.1155/2017/8738714 Epub 2017 Feb 1. PubMed PMID: 28255464; PubMed Central PMCID: PMC5309400.

[18] C.J. Lin, F.C. Chang, K.H. Chou, P.C. Tu, Y.H. Lee, C.P. Lin, P.N. Wang, I.H. Lee, Intervention versus aggressive medical therapy for cognition in severe asymptomatic carotid stenosis, AJNR Am. J. Neuroradiol. (2016) April 28. [Epub ahead of print] PubMed PMID: 27127004.

[19] T. Wang, D. Sun, Y. Liu, et al., The impact of carotid artery stenting on cerebral perfusion, functional connectivity, and cognition in severe asymptomatic carotid stenosis patients, Front. Neurol. 8 (2017) 403, https://doi.org/10.3389/fneur.2017.00403.

[20] R.L. Buckner, J.R. Andrews-Hanna, D.L. Schacter, The brain's default network: anatomy, function, and relevance to disease, Ann. N. Y. Acad. Sci. 1124 (March) (2008) 1–38, https://doi.org/10.1196/annals.1440.011 Review. PubMed PMID: 18400922.

[21] R.N. Spreng, W.D. Stevens, J.P. Chamberlain, A.W. Gilmore, D.L. Schacter, Default network activity, coupled with the frontoparietal control network, supports goal-directed cognition, NeuroImage. 53 (1) (2010) 303–317, https://doi.org/10.1016/j.neuroimage.2010.06.016.

[22] S.A. Julious, Sample size of 12 per group rule of thumb for a pilot study, Pharmaceut. Statist. 4 (2005) 287–291, https://doi.org/10.1002/pst.185.

[23] J.D. Kakisis, E.D. Avgerinos, C.N. Antonopoulos, T.G. Giannakopoulos, K. Moulakakis, C.D. Liapis, The European Society for Vascular Surgery guidelines for carotid intervention: an updated independent assessment and literature review, Eur. J. Vasc. Endovasc. Surg. 44 (September (3)) (2012) 238–243, https://doi.org/10.1016/j.ejvs.2012.04.015 Epub 2012 Jun 1. Review. PubMed PMID: 22658616.

[24] J.C. van Swieten, P.J. Koudstaal, M.C. Visser, H.J. Schouten, J. van Gijn, Interobserver agreement for the assessment of handicap in stroke patients, Stroke. 19 (May (5)) (1988) 604–607 PubMed PMID: 3363593.

[25] M.F. Folstein, S.E. Folstein, P.R. McHugh, Mini-mental state". A practical method for grading the cognitive state of patients for the clinician, J Psychiatr Res. 12 (November (3)) (1975) 189–198 PubMed PMID: 1202204.

[26] E. Magni, G. Binetti, A. Bianchetti, R. Rozzini, M. Trabucchi, Mini-mental state examination: a normative study in Italian elderly population, Eur. J. Neurol. 3 (May (3)) (1996) 198–202, https://doi.org/10.1111/j.1468-1331.1996.tb00423.x PubMed PMID: 21284770.

[27] H. Yamauchi, H. Fukuyama, Y. Nagahama, T. Shiozaki, S. Nishizawa, J. Konishi, H. Shio, J. Kimura, Brain arteriolosclerosis and hemodynamic disturbance may induce leukoaraiosis, Neurology 53 (Noember (8)) (1999) 1833–1838 PubMed PMID: 10563635.

[28] S. Whitfield-Gabrieli, A. Nieto-Castanon, Conn: a functional connectivity toolbox for correlated and anticorrelated brain networks, Brain Connect. 2 (3) (2012) 125–141, https://doi.org/10.1089/brain.2012.0073 Epub 2012 Jul 19. PubMed PMID: 22642651.

[29] R. Qi, L. Zhang, S. Wu, J. Zhong, Z. Zhang, Y. Zhong, L. Ni, Z. Zhang, K. Li, Q. Jiao, X. Wu, X. Fan, Y. Liu, G. Lu, Altered resting-state brain activity at functional MR imaging during the progression of hepatic encephalopathy, Radiology 264 (July (1)) (2012) 187–195, https://doi.org/10.1148/radiol.12111429 Epub 2012 Apr 16. PubMed PMID: 22509052.

[30] N. Fallon, Y. Chiu, T. Nurmikko, A. Stancak, Functional connectivity with the default mode network is altered in fibromyalgia patients, PLoS One 11 (July (7)) (2016) e0159198, https://doi.org/10.1371/journal.pone.0159198 eCollection 2016. PubMed PMID: 27442504; PubMed Central PMCID: PMC4956096.

[31] N. Makris, J.M. Goldstein, D. Kennedy, S.M. Hodge, V.S. Caviness, S.V. Faraone, M.T. Tsuang, L.J. Seidman, Decreased volume of left and total anterior insular lobule in schizophrenia, Schizophr. Res. 83 (April (2-3)) (2006) 155–171.

[32] J.A. Frazier, S. Chiu, J.L. Breeze, N. Makris, N. Lange, D.N. Kennedy, M.R. Herbert, E.K. Bent, V.K. Koneru, M.E. Dieterich, S.M. Hodge, S.L. Rauch, P.E. Grant, B.M. Cohen, L.J. Seidman, V.S. Caviness, J. Biederman, Structural brain magnetic resonance imaging of limbic and thalamic volumes in pediatric bipolar disorder, Am. J. Psychiatry 162 (July (7)) (2005) 1256–1265.

[33] R.S. Desikan, F. SÈgonne, B. Fischl, B.T. Quinn, B.C. Dickerson, D. Blacker, R.L. Buckner, A.M. Dale, R.P. Maguire, B.T. Hyman, M.S. Albert, R.J. Killiany, An automated labeling system for subdividing the human cerebral cortex on MRI scans into gyral based regions of interest, Neuroimage. 31 (July (3)) (2006) 968–980.

[34] J.M. Goldstein, L.J. Seidman, N. Makris, T. Ahern, L.M. O'Brien, V.S. Caviness Jr, D.N. Kennedy, S.V. Faraone, M.T. Tsuang, Hypothalamic abnormalities in schizophrenia: sex effects and genetic vulnerability, Biol. Psychiatry 61 (April (8)) (2007) 935–945.

[35] N. Tzourio-Mazoyer, B. Landeau, D. Papathanassiou, F. Crivello, O. Etard, N. Delcroix, B. Mazoyer, M. Joliot, Automated anatomical labeling of activations in SPM using a macroscopic anatomical parcellation of the MNI MRI single-subject brain, NeuroImage 15 (2002) 273–289.

[36] A.R. Laird, S.B. Eickhoff, K. Li, D.A. Robin, D.C. Glahn, P.T. Fox, Investigating the functional heterogeneity of the default mode network using coordinate-based meta-analytic modeling, J. Neurosci. 29 (46) (2009) 14496, https://doi.org/10.1523/JNEUROSCI.4004-09.2009.

[37] M. Schaaf, G. Mommertz, A. Ludolph, S. Geibprasert, G. Mühlenbruch, M. Das, T. Krings, Functional MR imaging in patients with carotid artery stenosis before and after revascularization, AJNR Am. J. Neuroradiol. 31 (November (10)) (2010) 1791–1798, https://doi.org/10.3174/ajnr.A2219 Epub 2010 Aug 26. PubMed PMID: 20801766.

[38] V. Axelrod, G. Rees, M. Bar, The default network and the combination of cognitive processes that mediate self-generated thought, Nat. Hum. Behav. 1 (2017) 896–910, https://doi.org/10.1038/s41562-017-0244-9.

[39] M. Konishi, D.G. McLaren, H. Engen, J. Smallwood, Shaped by the past: the default mode network supports cognition that is independent of immediate perceptual input. Hayasaka S, ed, PLoS One 10 (6) (2015) e0132209, , https://doi.org/10.1371/journal.pone.0132209.

[40] V. Smith, D.J. Mitchell, J. Duncan, Role of the default mode network in cognitive transitions, Cereb. Cortex (July) (2018), https://doi.org/10.1093/cercor/bhy167 [Epub ahead of print] PubMed PMID: 30060098.

[41] F.M. Krienen, R.L. Buckner, Segregated fronto-cerebellar circuits revealed by intrinsic functional connectivity, Cereb. Cortex 19 (10) (2009) 2485–2497, https://doi.org/10.1093/cercor/bhp135.

[42] K.R. Ridderinkhof, M. Ullsperger, E.A. Crone, S. Nieuwenhuis, The role of the medial frontal cortex in cognitive control, Science. 306 (October (5695)) (2004) 443–447 Review. PubMed PMID: 15486290.